Article

Spectroscopic Consequences of a Mixed Valence Excited State: Quantitative Treatment of a Dihydrazine Diradical Dication

Jenny V. Lockard, Jeffrey I. Zink, Asgeir E. Konradsson, Michael N. Weaver, and Stephen F. Nelsen

J. Am. Chem. Soc., **2003**, 125 (44), 13471-13480• DOI: 10.1021/ja036046k • Publication Date (Web): 08 October 2003

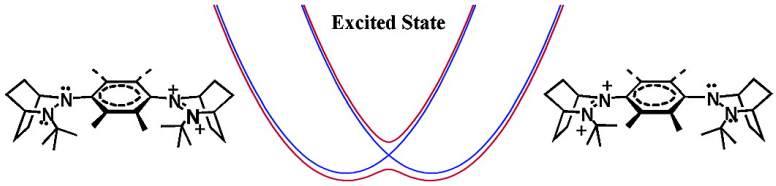

More About This Article

Additional resources and features associated with this article are available within the HTML version:

- Supporting Information
- Links to the 9 articles that cite this article, as of the time of this article download
- Access to high resolution figures
- Links to articles and content related to this article
- Copyright permission to reproduce figures and/or text from this article

View the Full Text HTML

J|A|C|S
ARTICLES
Published on Web 10/08/2003

Spectroscopic Consequences of a Mixed Valence Excited State: Quantitative Treatment of a Dihydrazine Diradical Dication

Jenny V. Lockard,[†] Jeffrey I. Zink,*[,†] Asgeir E. Konradsson,[‡] Michael N. Weaver,[‡] and Stephen F. Nelsen*[,‡]

Contribution from the Department of Chemistry and Biochemistry, University of California, Los Angeles, California 90095, and Department of Chemistry, University of Wisconsin, 1101 University Avenue, Madison, Wisconsin 53706-1396

Received May 9, 2003; E-mail: zink@chem.ucla.edu; nelsen@chem.wisc.edu

Abstract: A model for the quantitative treatment of molecular systems possessing mixed valence excited states is introduced and used to explain observed spectroscopic consequences. The specific example studied in this paper is 1,4-bis(2-*tert*-butyl-2,3-diazabicyclo[2.2.2]oct-3-yl)-2,3,5,6-tetramethylbenzene-1,4-diyl dication. The lowest energy excited state of this molecule arises from a transition from the ground state where one positive charge is associated with each of the hydrazine units, to an excited state where both charges are associated with one of the hydrazine units, that is, a Hy-to-Hy charge transfer. The resulting excited state is a Class II mixed valence molecule. The electronic emission and absorption spectra, and resonance Raman spectra, of this molecule are reported. The lowest energy absorption band is asymmetric with a weak low-energy shoulder and an intense higher energy peak. Emission is observed at low temperature. The details of the absorption and emission spectra are calculated for the coupled surfaces by using the time-dependent theory of spectroscopy. The calculations are carried out in the diabatic basis, but the nuclear kinetic energy is explicitly included and the calculations are exact quantum calculations of the model Hamiltonian. Because the transition involves the transfer of an electron from the hydrazine on one side of the molecule to the hydrazine on the other side and vice versa, the two transitions are antiparallel and the transition dipole moments have opposite signs. Upon transformation to the adiabatic basis, the dipole moment for the transition to the highest energy adiabatic surface is nonzero, but that for the transition to the lowest surface changes sign at the origin. The energy separation between the two components of the absorption spectrum is twice the coupling between the diabatic basis states. The bandwidths of the electronic spectra are caused by progressions in totally symmetric modes as well as progressions in the modes along the coupled coordinate. The totally symmetric modes are modeled as displaced harmonic oscillators; the frequencies and displacements are determined from resonance Raman spectra. The absorption, emission, and Raman spectra are fit simultaneously with one parameter set. The coupling in the excited electronic state H_{ab}^{ex} is 2000 cm^{-1}. Excited-state mixed valence is expected to be an important contributor to the electronic spectra of many organic and inorganic compounds. The energy separations and relative intensities enable the excited-state properties to be calculated as shown in this paper, and the spectra provide new information for probing and understanding coupling in mixed valence systems.

Introduction

Excited-state mixed valence occurs when an excited electronic state has two or more interchangeably equivalent sites with different oxidation states. The ground electronic state corresponds to a nondegenerate symmetrical charge distribution, in this work, an M^+-B-M^+ molecule where M is a redox active charge bearing unit such as the substituted hydrazine unit considered here, and B is a bridging unit, typically an aromatic system. The mixed valence excited electronic state for this case has two localized configurations: $M^{2+}-B-M^0$ and M^0-B-M^{2+}. Because the two charge-bearing units are coupled to each other, the excited state can be modeled in a manner similar to that of the familiar ground-state intervalence problem. The spectroscopy, however, is significantly different because the electronic transitions occur from the M^+-B-M^+ ground state to the coupled $M^{2+}-B-M^0/M^0-B-M^{2+}$ excited states, whereas for ground-state intervalence the transitions occur within the coupled M^+-B-M^0/M^0-B-M^+ system. Excited-state mixed valence can exist in both organic and inorganic molecules. For example, the lowest energy excited state of $Ru(bpy)_3^{2+}$ corresponds to metal-to-ligand charge transfer,[1] and each ligand can act as the charge-bearing unit in the excited state $[Ru^{3+}(bpy^-)(bpy)_2]^{2+}$. This system therefore provides an example of excited-state mixed valence, although its absorption spectrum has not

[†] University of California.
[‡] University of Wisconsin.

(1) Demandis, K. D.; Hartshorn, C. M.; Meyer, T. J. *Chem. Rev.* **2001**, *101*, 2655.

10.1021/ja036046k CCC: $25.00

Scheme 1. Reversible First Electron and Irreversible Second Electron Loss from **ArHy** Caused by *tert*-Butyl Cleavage from the Dication

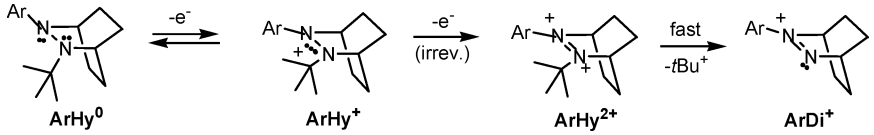

been analyzed in these terms. The new spectroscopic features that arise from the ground to coupled excited-state transition, and the information that can be obtained from the spectra, are the subject of this paper.

The principal compound studied here is the durenediyl (**DU**)-bridged dihydrazine diradical dication $\mathbf{1}^{2+}$, which has 2-*tert*-butyl-2,3-diazabicyclo[2.2.2]oct-3-yl (**Hy**) charge-bearing units.

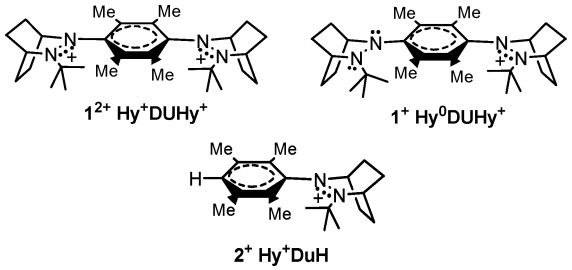

In contrast to the monocation oxidation level $\mathbf{1}^{+}Ph_4B^{-}$, which has been shown by X-ray crystallography to have essentially complete charge localization on one $\mathbf{Hy}^{+}$ unit, and may be symbolized as $\mathbf{Hy^0DUHy}^{+}$, the hydrazine units of $\mathbf{1}^{2+}$ are both oxidized and have been shown by X-ray crystallography of the $(Ph_4B^{-})_2$ salt to be related by a crystallographic C_2 axis.[2] There are significant differences between the geometries of oxidized and reduced **Hy** units. The $\mathbf{Hy^0}$ unit nitrogens of $\mathbf{1}^{+}Ph_4B^{-}$ each bear a lone pair electron and have NN distances of 1.44−1.46 Å. Their N*t*Bu and NAr nitrogens deviate from planarity with $\Delta\alpha_{av} = 6-8°$ and 6−7°, respectively.[3] The $\mathbf{Hy}^{+}$ units share three π electrons on two nitrogens, causing a significantly shorter NN distance, 1.35 and 1.36 Å for the mono- and dication, respectively. The $\mathbf{Hy}^{+}$ nitrogens are also considerably less pyramidal, $\Delta\alpha_{av} = 1.4°$ and 1.0°, respectively, for $\mathbf{1}^{+}Ph_4B^{-}$, and 1.5° and 1.5°, respectively, for $\mathbf{1}^{2+}(Ph_4B^{-})_2$. Thus, a relatively large geometry change accompanies electron transfer from $\mathbf{Hy^0}$ to $\mathbf{Hy}^{+}$ in $\mathbf{1}^{+}$, and hence it has a large vertical reorganization energy, λ, causing its absorption maximum to occur in the visible instead of the near-IR region, where localized intervalence compounds having smaller λ values occur. Scheme 1 shows what occurs when a second electron is removed from $\mathbf{ArHy}^{+}$.

Although the first electron removal is reversible because the radical cation is long-lived, second electron removal to give $\mathbf{ArHy}^{2+}$ is effectively irreversible because the dication is very short-lived, rapidly cleaving a *tert*-butyl cation to give the aryldiazenium cation, $\mathbf{ArDi}^{+}$.[4] The irreversibility of the second oxidation makes the formal potential for $\mathbf{ArHy}^{+/2+}$ difficult to estimate accurately. However, the second electron is 1.39 V harder to remove than the first for the tetra-secondary alkyl substituted bis-bicyclic hydrazine **3**, for which 0, 1+, and 2+ oxidation states are isolable and the measurement may be made accurately by cyclic voltammetry.[5] Thirteen examples of *N*,*N*′-

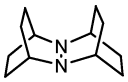

3

bis-bicyclic hydrazines that have two reversible oxidation waves have 1+/2+, 0/1+ formal potential differences in the range from 0.94 to 1.66 V.[6] Intramolecular electron-transfer disproportionation that converts ground-state $\mathbf{1}^{2+}$ ($^{+}\mathbf{HyDUHy}^{+}$) to ($^{2+}\mathbf{HyDUHy^0}$), an excited-state electronic configuration, is therefore expected to be approximately 1−1.5 eV endoenergetic and will only occur very slowly thermally. The present work includes comparisons of the optical absorption spectra of $\mathbf{1}^{+}$ and $\mathbf{1}^{2+}$, which were discussed in a previous communication.[7] It was pointed out that the position and intensity of the $\mathbf{1}^{2+}$ lowest energy absorption band were qualitatively consistent with its assignment as intramolecular electron-transfer disproportionation and that the ratio of the electronic coupling determined using the Hush Gaussian band shape approximation to its transition energy is consistent with the observed singlet, triplet energy gap.

Electronic transitions to mixed valence excited states are treated quantitatively in this paper using the time-dependent theory of spectroscopy[8−12] specifically applied to coupled electronic states.[13,14] The original application of the theory was to intensity borrowing caused by coupled states. A spin forbidden absorption band borrows intensity from a spin allowed band because of spin−orbit coupling between the two electronic excited states.[15] A wave packet that is produced on the allowed excited-state potential surface transfers amplitude to the forbidden state surface. The detailed vibronic structure is dependent on the energy separations, the positions of the minima of the states along vibrational coordinates, and the magnitude of the spin−orbit coupling. Another type of application treated the absorption and emission spectra of coupled states in transition metal compounds.[16−18] The spectra were interpreted in terms

(2) (a) Nelsen, S. F.; Ismagilov, R. F.; Powell, D. R. *J. Am. Chem. Soc.* **1997**, *119*, 10213. (b) The orientation of the $\mathbf{Hy^0}$ units with respect to $\mathbf{Hy}^{+}$ does not affect the energy significantly, and three orientations of the neutral hydrazines relative to the oxidized one were detected in the crystal.
(3) $\Delta\alpha_{av} = 120 -$ (average of the bond angles at nitrogen), and varies from 0° for a planar nitrogen to 10.5° for a nitrogen that is tetrahedral.
(4) Nelsen, S. F.; Parmelee, W. P. *J. Org. Chem.* **1981**, *46*, 3453.
(5) (a) Nelsen, S. F.; Blackstock, S. C.; Frigo, T. B. *J. Am. Chem. Soc.* **1984**, *106*, 3366. (b) Nelsen, S. F.; Blackstock, S. C.; Haller, K. J. *Tetrahedron* **1986**, *42*, 6101.
(6) Nelsen, S. F.; Frigo, T. B.; Kim, Y. *J. Am. Chem. Soc.* **1989**, *111*, 5387.
(7) Nelsen, S. F.; Ismagilov, R. F.; Powell, D. R. *J. Am. Chem. Soc.* **1998**, *120*, 2200.
(8) Lee, S.-Y.; Heller, E. J. *J. Chem. Phys.* **1979**, *71*, 4777.
(9) Heller, E. J. *Acc. Chem. Res.* **1981**, *14*, 368.
(10) Heller, E. J.; Sundberg, R. L.; Tannor, D. *J. Phys. Chem.* **1982**, *86*, 1822.
(11) Myers, A. B. *Laser Techniques in Chemistry*; Wiley: New York, 1995; Vol. 23, p 325.
(12) Zink, J. I.; Shin, K.-S. K. *Advances in Photochemistry*; Wiley: New York, 1991; Vol. 16, p 119.
(13) Reber, C.; Zink, J. I. *Comments Inorg. Chem.* **1992**, *13*, 177.
(14) Wexler, D.; Zink, J. I.; Reber, C. In *Electronic and Vibronic Spectra of Transition Metal Complexes*; Yersin, I. H., Eds.; Springer-Verlag: Berlin, Heidelberg, 1994; p 174.
(15) Wexler, D.; Reber, C.; Zink, J. I. *J. Phys. Chem.* **1992**, *96*, 8757.
(16) Pelletier, Y.; Reber, C. *Inorg. Chem.* **1997**, *36*, 721.
(17) Bussière, G.; Reber, C. *J. Am. Chem. Soc.* **1998**, *120*, 6306.
(18) Bussière, G.; Beaulac, R.; Cardinal-David, B.; Reber, C. *Coord. Chem. Rev.* **2001**, *219*−*221*, 509.

of surfaces coupled along an asymmetric normal coordinate. A more complicated spectroscopic manifestation in electronic spectra of coupling between surfaces is the existence of interference dips, that is, the decrease of absorbance in a broad absorption band at the position of a second absorption band.[19−24] This phenomenon arises because of destructive interference between wave packets on the two coupled excited-state surfaces. It cannot be interpreted in terms of diabatic or adiabatic Born−Oppenheimer potential energy surfaces; the nuclear kinetic energy must be included. Intervalence electron-transfer spectroscopy is another example where Born−Oppenheimer potential energy surfaces are not sufficient. Intervalence spectra can be conveniently calculated and physically interpreted by using time-dependent theory and wave packet propagation on coupled surfaces,[25−27] but in this case the transitions occur within the two coupled states and not from a third (ground) state to the coupled system.

In this paper, we introduce an excited-state mixed valence potential energy surface model to explain the features of the absorption and emission bands of the durene-bridged bishydrazine dication, $\mathbf{1}^{2+}$. The experimental absorption spectrum consists of a dominant peak with a less intense shoulder at lower energy. Both the shoulder and the peak are a consequence of the transition to the coupled excited state. In fitting the spectrum, both the separation between the peak maximum and the shoulder as well as the intensity ratio of the two are determined by the coupling between the excited-state surfaces in the model. Emission from the lowest energy vibronic level of the coupled excited state to the ground state is observed at low temperature. The displacements of the excited-state coupled surfaces along the asymmetric coordinate are predominantly responsible for the bandwidth of the emission spectrum. Symmetric modes also play an important role in fitting both the emission and the absorption spectra. Resonance Raman spectra are used to determine the frequencies and displacements of the totally symmetric normal modes. The electronic spectra are calculated by using the time-dependent theory of spectroscopy and methodology designed to calculate spectra involving coupled surfaces. The parameters that define these coupled surfaces are examined, and the treatment of the dipole moment for transitions to these surfaces is discussed in detail. The absorption, emission, and Raman spectra are fit simultaneously with one parameter set and include progressions in the totally symmetric modes as well as progressions in the modes involving the coupled coordinate.

Experimental Section

Infrared Spectroscopy. Mid-IR spectra of $\mathbf{1}^{2+}$ were taken of a CsI pellet on a Mattson Polaris IR spectrometer with a resolution of 1 cm^{-1}. The data were collected using a PC. Far-IR spectra were taken of a CsI pellet on a Nicolet Nexus spectrometer with a 4 cm^{-1} resolution.

Raman Spectroscopy. Spectra were obtained using a 1401 Spex double monochromator equipped with a Burle C31034 photomultiplier tube. Data were collected using a Stanford Research System SR400 photon counter and processed by a PC computer. The 676, 647, 568, 530, and 482 nm lines of a Coherent I-300 Krypton laser at ∼100 mW were used for excitation. The dication sample was mixed with potassium nitrate standard in a pressed pellet, and all of the spectra were collected from a spinning sample cooled by a stream of nitrogen gas to limit thermal heating from the laser.

Emission Spectroscopy. Emission spectra taken at 15 K were obtained using a Spex 1702 single monochromator equipped with an S1 photomultiplier tube. The signal was recorded with a Stanford Research System SR400 photon counter and processed by a computer. The 406 nm line of a Coherent I-300 Krypton laser at 4 mW was used for excitation. The solid sample was cooled using an Air Products closed cycle helium refrigerator displex equipped with a thermocouple. The spectrum was corrected for instrument response.

Theoretical and Numerical Methods

The theoretical foundation underlying the calculation of electronic spectra for coupled potential surfaces in the framework of the time-dependent theory of molecular spectroscopy is briefly presented in this section. The time-dependent approach is very powerful from both technical and conceptual points of view.[8−10,28] Its utility is particularly evident in the treatment of coupled electronic states. In the Franck−Condon picture, the spectroscopic consequences of coupling between states are much harder to visualize qualitatively and to calculate quantitatively than with time-dependent methods.

Absorption Spectra. The fundamental equation for the calculation of an absorption spectrum in the time-dependent theory is

$$I(\omega) = C\omega \int_{-\infty}^{+\infty} \exp(i\omega t)\left\{\langle\Phi|\Phi(t)\rangle \exp\left(-\Gamma^2 t^2 + \frac{iE_0}{h}t\right)\right\} \mathrm{d}t \quad (1)$$

with $I(\omega)$ as the absorbance at frequency ω, E_0 as the energy of the electronic origin transition, and Γ as a phenomenological Gaussian damping factor.[12] The damping factor arises because of relaxation into other modes (such as low-frequency solvent modes with small distortions) and the "bath". The effect of increasing Γ on the spectrum in the frequency domain is to decrease the resolution, that is, to "fill in" the spectrum.

The most important part of eq 1 is $\langle\Phi|\Phi(t)\rangle$, the autocorrelation function of the wave packet Φ prepared on an excited-state potential surface after the spectroscopic transition, with the wave packet $\Phi(t)$ developing on this surface with time. In the absence of coupling terms between the normal coordinates, the total autocorrelation in a system with K coordinates is given by

$$\langle\Phi|\Phi(t)\rangle = \prod_k \langle\phi^k|\phi^k(t)\rangle \quad (2)$$

where ϕ^k is a wave packet associated with coordinate k (k = 1,..., K) and is a two-dimensional vector: $\phi^k(Q_k,j)$, where Q_k is the coordinate along mode K, and j = 1,2 is an index over the two electronic states. In the following, we will eliminate the index k and consider only a single coordinate. The t = 0 wave packet is then defined as

(19) Reber, C.; Zink, J. I. *J. Chem. Phys.* **1992**, *96*, 2681.
(20) Neuhauser, D.; Park, T. J.; Zink, J. I. *Phys. Rev. Lett.* **2000**, *85*, 5304.
(21) Landry-Hum, J.; Tessier, V.; Ernzerhof, M.; Reber, C. *Coord. Chem. Rev.* **2002**, 233−*234*, 65.
(22) Schenker, R.; Triest, M.; Reber, C.; Güdel, H. U. *Inorg. Chem.* **2001**, *40*, 5787.
(23) Bussiere, G.; Reber, C.; Neuhauser, D.; Walter, D. A.; Zink, J. I. *J. Phys. Chem. A* **2003**, *107*, 1258.
(24) Reber, C.; Zink, J. I. *J. Phys. Chem.* **1992**, *96*, 571
(25) Simoni, E.; Reber, C.; Talaga, D.; Zink, J. I. *J. Phys. Chem.* **1993**, *97*, 12678.
(26) Talaga, D. S.; Zink, J. I. *J. Phys. Chem.* **1996**, *100*, 8712.
(27) Talaga, D. S.; Zink, J. I. *J. Phys. Chem. A* **2001**, *105*, 10511.
(28) Zhang, J. Z.; Heller, E. J.; Huber, D.; Imre, D. G. *J. Phys. Chem.* **1991**, *95*, 6129.

$$\phi(t=0) = \mu\chi_i \tag{3}$$

or more explicitly:

$$\phi(Q,j,t=0) = \sum_{j=1}^{2} \mu_j(Q)\chi_i(Q) \tag{4}$$

Here, the subscript "i" denotes the initial state; χ_i is the lowest energy ground-state eigenfunction. We do not label ϕ by the initial state index i to avoid cluttering with indices, but the wave packet depends on the initial state. The signs of the transition dipole moments μ_j ($j = 1,2$) depend on the direction of the electron transfer and are opposite for the antiparallel transitions in the molecule discussed in this paper. The diagonal elements, H_j, of the Hamiltonian are

$$H_j = -\frac{1}{2M}\nabla^2 + V_j(Q) \tag{5}$$

where $V_j(Q)$ is the potential energy as a function of the configurational coordinate Q, and $-\nabla^2/(2M)$ is the nuclear kinetic energy.

When two coupled surfaces that represent the excited state are involved, we need to keep track of two wave packets, ϕ_1 and ϕ_2, moving on the two coupled potential surfaces.[29−31] The wave packet $\phi(t)$ is given by the time-dependent Schrödinger equation:

$$i\frac{\partial}{\partial t}\begin{pmatrix}\phi_1\\ \phi_2\end{pmatrix} = \begin{pmatrix}H_1 & V_{12}\\ V_{21} & H_2\end{pmatrix}\begin{pmatrix}\phi_1\\ \phi_2\end{pmatrix} \tag{6}$$

where now the subscript denotes the electronic state, $j = 1$ or 2, the diagonal elements H_j of the total Hamiltonian are given in eq 5, and $V_{12} = V_{21}$ is the coupling between the two diabatic potentials and is intrinsically negative. The total overlap $\langle\phi|\phi(t)\rangle$ is calculated as

$$\langle\phi|\phi(t)\rangle = \langle\phi_1|\phi_1(t)\rangle + \langle\phi_2|\phi_2(t)\rangle \tag{7}$$

For simplicity, we chose harmonic potentials in all of the following examples, although the methods used are not restricted by the functional form of the potentials. The displacement of the minimum of one electronic state from the other, from that of the ground state, ΔQ, is abbreviated as Δ in this paper. The potentials are given by

$$V_j(Q) = \frac{1}{2}k_j(Q \pm \Delta Q_j)^2 + E_j \tag{8}$$

with $k_j = 4\pi^2 M(h\omega_i)^2$ as the force constant, ΔQ_j as the positions of the potential minima along Q, and E_j as the energy of the potential minimum for state j. These uncoupled potentials are shown in Figure 1 (dashed lines). The coupling between the diabatic potentials for states 1 and 2 is chosen to be coordinate independent in this paper, although the computational method allows us to use coordinate-dependent coupling. Note that different authors use the symbols for the coupling V_{12} or H_{ab} or ϵ interchangeably. The symbol H_{ab} is used in the remainder of this paper because H_{ab} is most commonly found in discussions of organic compounds. For excited states, the symbol H_{ab}^{ex} is used, and the superscript denotes coupling in the excited electronic state.

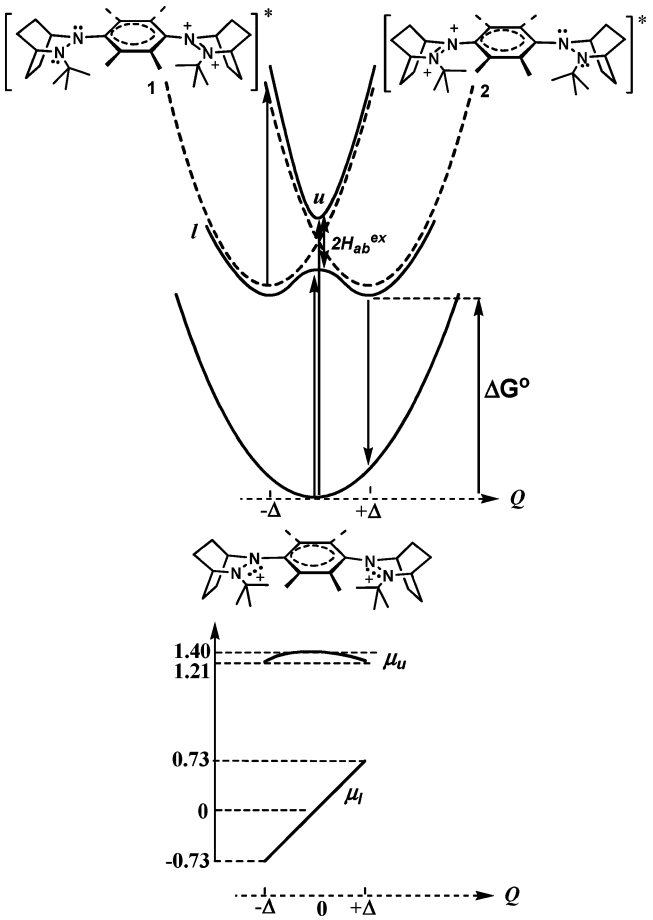

Figure 1. Potential energy surfaces as a function of an asymmetric coordinate. The lowest energy surface represents the ground electronic state. The pair of surfaces at higher energy represents the mixed valence excited electronic state. The solid lines are the adiabatic surfaces; the dotted lines are diabatic surfaces. The transition dipole moments for the adiabatic surfaces are plotted as a function of the vibrational coordinate below the surfaces. That for the upper adiabatic surface, μ_u, is always nonzero, but that for the lower adiabatic surface, μ_l, changes sign at the origin.

The configurational coordinate in Figure 1 requires further explanation. It is rarely defined precisely, in part because there are usually several possibilities and it is difficult to choose the most important one. The coordinate that is chosen here is an asymmetric mode with a vibrational energy of 1462 cm^{-1}.

Emission Spectra. The fundamental equation for the calculation of an emission spectrum in the time-dependent theory is similar to that for the absorption spectrum calculation:

$$I(\omega) = C\omega^3 \int_{-\infty}^{+\infty} \exp(i\omega t)\left\{\langle\Phi|\Phi(t)\rangle \exp\left(-\Gamma^2 t^2 + \frac{iE_0}{h}t\right)\right\} \mathrm{d}t \tag{9}$$

For emission spectroscopy, the wave packet originates from the coupled excited-state surfaces and is propagated on the ground-state surface. The calculation of the autocorrelation function, $\langle\phi|\phi(t)\rangle$, requires the appropriate initial wave packet, $\phi(t = 0)$, and by eq 3, χ_i, the lowest energy eigenfunction of the coupled excited-state surfaces. The eigenfunction has two components, one from each of the diabatic surfaces. The eigenfunction is calculated as follows:

(29) Alvarellos, J.; Metiu, H. *J. Phys. Chem.* **1988**, *92*, 4957.
(30) Jiang, X. P.; Heather, R.; Metiu, H. *J. Chem. Phys.* **1989**, *90*, 6903.
(31) Heather, R.; Metiu, H. *J. Chem. Phys.* **1992**, *96*, 2681.

$$\chi_i = \text{const.} \int_0^T \eta(t) w(t) \exp\left(\frac{iE_i}{h} t\right) dt \qquad (10)$$

where χ_i denotes the eigenfunction corresponding to the eigenvalue E_i, $\eta(t)$ is the time-dependent (propagating) wave function which initially is located arbitrarily on the surface, and $w(t)$ is a Hanning window function. Note that for coupled potentials, each eigenfunction χ_i is an array with two components corresponding to the two diabatic potentials that form the basis in the calculations; that is, χ_i is specifically $\chi_i(Q,j)$.

Results

1. Electronic Spectroscopy. The electronic spectra of $\mathbf{1}^{2+}$ are shown in Figure 2. The lowest energy absorption band of $\mathbf{1}^{2+}$ is asymmetric with a maximum at 22 420 cm^{-1} (446 nm) and a less intense shoulder at 17 200 cm^{-1} (581 nm). Higher energy absorption bands occur with peak maxima at 29 590, 35 590, and 39 370 cm^{-1}. The absorption of $\mathbf{1}^{+}$ in acetonitrile shows a broad maximum at 14 100 cm^{-1} (709 nm).[2a]

The low-temperature emission spectrum of the dication solid consists of an unstructured band with its maximum at 13 460 cm^{-1} (743 nm) and a full width at half-maximum of 2640 cm^{-1}.

2. Vibrational Spectroscopy. The observed resonance Raman frequencies (in wavenumbers) and the integrated intensities for those modes (normalized to the intensity of the 720 cm^{-1} peak from the KNO_3 standard) obtained using 482 nm excitation are as follows: 350 cm^{-1} (0.86); 1015 cm^{-1} (0.52); 1181 cm^{-1} (0.5); 1305 cm^{-1} (1.61); 1413 cm^{-1} (1.04); 1552 cm^{-1} (2.48). The bands listed have an intensity of at least 20% of that of the most intense band at 1552 cm^{-1}.

Discussion

1. Assignments of the Absorption Bands of $\mathbf{1}^{2+}$. The bands in the region of the lowest energy absorption band of $\mathbf{1}^{2+}$ (446 nm) are assigned to a transition from the ground state, where each hydrazine unit contains one positive charge, to a coupled excited state where both charges are located on one hydrazine unit. As pointed out previously,[7] the presence of the **Hy**-to-**Hy**$^+$ superexchange band in the intervalence oxidation level $\mathbf{1}^{+}$ implies that a **Hy**$^+$-to-**Hy**$^+$ band of similar intensity will occur for the $\mathbf{1}^{2+}$ oxidation level. The most convincing evidence to support this assignment, instead of a **B**-to-**Hy**$^+$ absorption, which will also occur in the same general region, comes from the saturated-bridged dihydrazine analogues of **1**, **4**, and **5**.[32] The

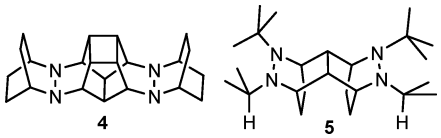

intervalence radical cation $\mathbf{4}^{+}$ has its **Hy**-to-**Hy**$^+$ superexchange band in acetonitrile at 16 290 cm^{-1} (614 nm, $\mu_{12} = 1.88$ D), while the diradical dication $\mathbf{4}^{2+}$ has its band maximum at 22 000 cm^{-1} (454 nm). The intervalence radical cation $\mathbf{5}^{+}$ has its **Hy**-to-**Hy**$^+$ band in acetonitrile at 18 000 cm^{-1} (556 nm, $\mu_{12} = 1.73$ D), while the diradical dication $\mathbf{5}^{2+}$ has its band maximum at 21 550 cm^{-1} (464 nm). Similar increases in band maxima between radical cation and dication occur for other alkyl substituted bishydrazines that have saturated bridges.[33] These compounds cannot reasonably have a bridge-centered cation formed with a low enough transition energy to occur in the region of the spectrum observed, so their longest wavelength bands can only be reasonably attributed to *ET* disproportionation.

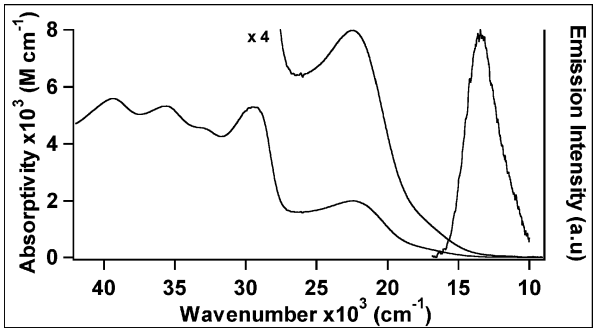

Figure 2. Electronic spectra of $\mathbf{1}^{2+}$. Left: Room-temperature absorption spectrum in an acetonitrile solution. Note the shoulder at about 17 000 cm^{-1}. Right: Solid-state luminescence spectrum at 10 K.

If the lowest energy transition for $\mathbf{1}^{2+}$ corresponds to **Hy**$^+$-to-**Hy**$^+$ superexchange, where does its **B**-to-**Hy**$^+$ band occur? The lowest energy transition for the monohydrazine analogue $\mathbf{2}^{+}$ occurs at 23 600 cm^{-1} (424 nm) and may be confidently assigned as **B**-to-**Hy**$^+$ *ET*. It is substantially lower in energy than the $\pi-\pi^*$ transition in either the aromatic system or the alkyl-substituted **HyR**$^+$.[34] Although this is only 1600 cm^{-1} higher in energy than the maximum for $\mathbf{1}^{2+}$, because the latter has a **DU** ring that is *para*-substituted by a **Hy**$^+$ group instead of a hydrogen, the **B**-to-**Hy**$^+$ *ET* for $\mathbf{1}^{2+}$ ought to occur at higher energy than 22 000 cm^{-1}. The $\pi-\pi^*$ transition in the monohydrazine cation $\mathbf{2}^{+}$ has a maximum at 30 300 cm^{-1} (330 nm), and $\mathbf{1}^{2+}$ also shows strong absorption in this region, which overlaps with the high-energy side of the *ET* disproportionation band (see Figure 2), but also presumably contains the **B**-to-**Hy**$^+$ absorption.

Figure 1 only considers the singlet state of the dication. Although the triplet state is present in a similar amount at room temperature because it is only about 70 cm^{-1} higher in energy,[7] its *ET* transitions will be significantly higher in energy than those of the singlet because excitation of the triplet must produce a triplet hydrazine dication, neutral hydrazine, or durene π system.

2. Excited-State Mixed Valence Model. The focus in this section is on two coupled potential energy surfaces along an asymmetric normal coordinate that represent excited-state mixed valence. The model is described in detail in part a, and appropriate parameters are discussed in part b.

a. Coupled Surfaces. The excited-state intervalence behavior of the symmetric molecule is modeled by two interacting harmonic potential energy surfaces in the excited state as shown in Figure 1. A single harmonic surface with its minimum at zero along the normal vibrational coordinate represents the ground state with equal charge on both sides of the molecule. Two possible electronic transitions that are in opposite directions create a separation of charge within the molecule. Symmetry requires that these transitions be equal in energy and occur with

(32) Nelsen, S. F.; Adamus, J.; Wolff, J. J. *J. Am. Chem. Soc.* **1994**, *116*, 1589.

(33) Nelsen, S. F.; Ramm, M. T.; Wolff, J. J.; Powell, D. R. *J. Am. Chem. Soc.* **1997**, *119*, 6863.

(34) Nelsen, S. F.; Tran, H. Q.; Ismagilov, R. F.; Chen, L.-J.; Powell, D. R. *J. Org. Chem.* **1998**, *63*, 2536.

equal probability. In the model, these energetically equal transitions give rise to two diabatic surfaces in the excited state (dashed lines) that are degenerate at $Q = 0$, each representing the system with the entire charge localized on one side of the molecule. The excited-state diabatics are displaced from the ground-state surface such that the Franck−Condon region of each diabatic has a nonzero slope that is equal in magnitude and opposite in sign. The diabatic surfaces couple, via the H_{ab}^{ex} coupling term, creating two new nondegenerate adiabatic surfaces (solid lines) with an energy splitting of $2H_{ab}^{ex}$ at $Q = 0$ between the lower and the higher energy adiabatic surfaces. These surfaces are depicted along an asymmetric normal coordinate. Vibration along this coordinate in the excited state brings the molecule from one intervalence extreme to the other. Wave packet propagation is discussed in section 3c.

b. Choosing Appropriate Parameters for the Coupled Surfaces. To calculate the absorption spectrum, first the appropriate frequency must be chosen for the asymmetric mode of the excited-state mixed valence surfaces. Selection rules for the dication, which is symmetric in its ground state, eliminate the Raman active modes as potential candidates for this frequency. Therefore, only frequencies of modes that are exclusively IR-active were considered in defining the ground- and excited-state surfaces along the asymmetric coordinate. From the experimental IR data, we chose the 1462 cm^{-1} frequency to define the ground-state harmonic potential surface. This choice is reasonable because the **Hy**-to-**Hy** transition is expected to involve an asymmetric N−N or C−N stretching mode and a large change in the bond length. Based on molecular orbital calculations of similar molecules, asymmetric normal coordinates involving significant C−N−N displacements occur at about this frequency. In the excited state, the displaced diabatic surfaces couple, and the resulting coupled system has different vibrational frequencies. These frequencies are determined by H_{ab}^{ex} and the diabatic potentials' frequencies and displacements. Therefore, these parameters are chosen such that the appropriate vibrational frequency is produced. Additional constraints on choosing the frequency will be discussed in section 3a.

The displacement of these surfaces along the vibrational normal coordinate is also crucial for the absorption spectrum calculation. The dimensionless displacement, Δ, is directly related to the bond length changes within the molecule that occur upon excitation. For the best fit, a Δ value of 1.55 was determined.

3. Absorption Spectra for Transitions from the Ground to the Mixed Valence Excited States. In this section, the calculated absorption spectrum arising from the **Hy**-to-**Hy** transition is discussed. In part a, the effect of the coupling on the band shape is explored. In part b, a simple explanation for the intensities is derived. The time-dependent interpretation is discussed in section c.

a. Calculated Absorption Spectra. The absorption spectrum of the dication, as shown in Figure 2, reveals the effects of coupling along this asymmetric coordinate in the excited state. The peak at 22 420 cm^{-1} and shoulder to lower energy correspond to the transition to the upper and lower adiabatic surface, respectively. The difference in energy between the peak maximum and shoulder, therefore, is directly related to the coupling along the asymmetric coordinate involved in the excited state. If the coupling had been zero, a single peak (with no shoulder) would be observed in the absorption spectrum because the transition to one diabatic surface produces the same spectrum as a transition to the other.

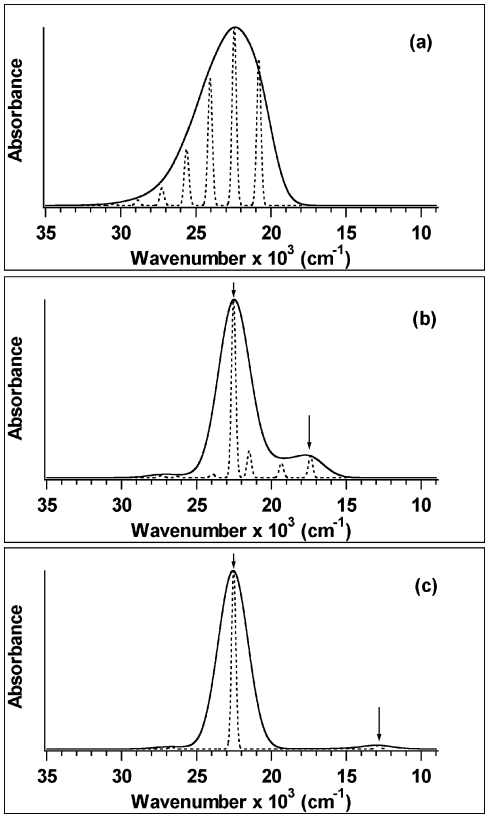

Figure 3. Calculated absorption spectra as a function of the coupling H_{ab}^{ex} between the diabatic excited-state potential energy surfaces. The values of the coupling are (a) $H_{ab}^{ex} = 100$ cm^{-1}, (b) $H_{ab}^{ex} = 2000$ cm^{-1}, and (c) $H_{ab}^{ex} = 5000$ cm^{-1}.

The experimental absorption spectrum for the dication system determines the coupling value, H_{ab}^{ex}, between the two excited-state diabatic surfaces. For example, as illustrated in Figure 3b, when a H_{ab}^{ex} value of 2000 cm^{-1} is used to calculate the absorption spectrum, the energy difference between the two peaks of the calculated spectrum matches the energy difference between the shoulder and peak maximum of the experimental spectrum. To illustrate the effect of changing the coupling on the spectrum, two extreme values of coupling were used. When a H_{ab}^{ex} value of 100 cm^{-1} was used, Figure 3a, the spectrum is reduced to a single band with no shoulder. In this case, the coupling used in the calculation is too small. When H_{ab}^{ex} equals 5000 cm^{-1}, Figure 3c, the resulting calculated absorption spectrum has a peak separation that is too large to fit the experimental spectrum. For all of these spectra, $\Delta = 1.55$.

The absorption spectrum is less influenced by the frequency of the asymmetric mode than it is by the coupling. For example, a low-frequency mode such as a C−N bending mode could be involved. To illustrate this point, a 521 cm^{-1} mode observed in the IR spectrum is chosen. The coupling, $H_{ab}^{ex} = 2000$ cm^{-1}, remains the same as that in the high-frequency example illustrated in Figure 3b. The value of Δ is different. A spectrum similar to that in Figure 3b is calculated by using $\Delta = 4.69$ as shown in Figure 4b. This result shows that the absorption spectrum alone does not allow the discrimination between the low- and high-frequency modes as the important mode. How-

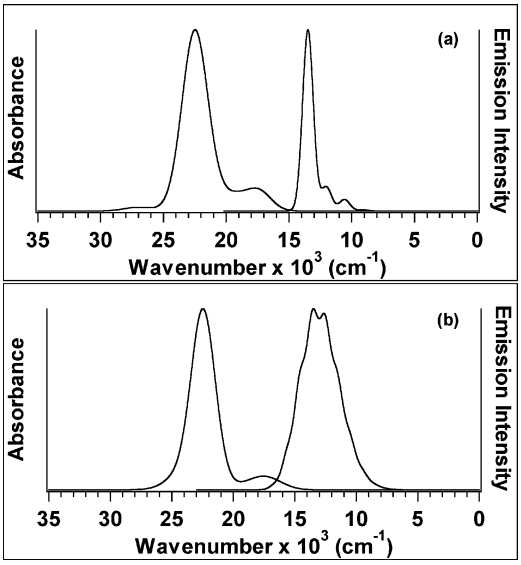

Figure 4. Absorption and emission spectra calculated for potential surfaces with high and low vibrational frequencies. Top: Calculated absorption spectrum using a high-frequency (1600 cm^{-1}) vibrational mode. The corresponding calculated emission spectrum is shown at the right. Bottom: Calculated absorption spectrum using a low-frequency (521 cm^{-1}) vibrational mode. The corresponding calculated emission spectrum (right) is significantly broader than the experimental spectrum.

ever, as will be shown in section 4, the emission spectrum is very sensitive to the vibrational frequency and does provide severe constraints on the choice of the active mode.

b. The Transition Dipole Moments. The trends in the intensities of the low-energy and high-energy components of the absorption band are most easily explained in terms of the transition dipole moment μ. In all of the calculations, it is assumed that the Condon approximation is valid and that μ is a constant independent of the normal coordinate. In accord with the calculation procedures described in the Theoretical and Numerical Methods section, the initial wave packet $\mu\chi(t = 0)$ is placed on both excited-state diabatic surfaces and propagated with the coupling included at each time step. If the coupling is zero, the spectrum is similar to that of the familiar displaced harmonic oscillator electronic spectrum but with an absorbance twice that from a single displaced potential.

In the case of the dication discussed in this paper, μ has opposite signs for the transitions to the two diabatic basis surfaces. In the coordinate system of Figure 1, for example, the transition dipole moment corresponds to the electron moving to the left for the surface with its minimum $Q = -\Delta$ and vice versa. The two dipole moments are antiparallel.

The dipole moment matrix in the diabatic basis that represents the transition from the ground state to the two diabatic states is

$$\mu_d = \begin{pmatrix} 0 & -\mu_1 & \mu_2 \\ -\mu_1 & 0 & 0 \\ \mu_2 & 0 & 0 \end{pmatrix} \tag{11}$$

The transformation to the adiabatic basis $U^{-1}\mu_d U = \mu_a$ uses the transformation matrix

$$U^{-1} = \begin{pmatrix} 1 & 0 & 0 \\ 0 & \cos\vartheta & \sin\vartheta \\ 0 & -\sin\vartheta & \cos\vartheta \end{pmatrix} \tag{12}$$

where

$$\tan 2\vartheta = \frac{2H_{ab}^{ex}}{V_1(Q) - V_2(Q)} \tag{13}$$

The transition dipole moment matrix in the adiabatic basis is

$$\mu_a = \begin{pmatrix} 0 & \mu_2 \sin\vartheta - \mu_1 \cos\vartheta & \mu_1 \sin\vartheta + \mu_2 \cos\vartheta \\ \mu_2 \sin\vartheta - \mu_1 \cos\vartheta & 0 & 0 \\ \mu_1 \sin\vartheta + \mu_2 \cos\vartheta & 0 & 0 \end{pmatrix} \tag{14}$$

In the adiabatic basis, the transition dipole to the upper surface, $\mu_u = \mu_1 \sin\vartheta + \mu_2 \cos\vartheta$, is nonzero everywhere along the Q coordinate. The physical meaning is that the transition from the ground state to the upper adiabatic state (in the adiabatic limit where $H_{ab}^{ex} \gg V_1(Q) - V_2(Q)$) is electric dipole allowed. In contrast, the transition dipole to the lower adiabatic state is $\mu_l = \mu_2 \sin\vartheta - \mu_1 \cos\vartheta$. This function is zero at $Q = 0$ but is positive when $Q > 0$ and negative when $Q < 0$ (see the lower portion of Figure 1 for a diagram illustrating how μ_u and μ_l change with Q). The physical meaning is that the transition is electric dipole forbidden at the internuclear equilibrium geometry but is vibronically allowed.

It is important to reiterate that the calculations of the spectra include the nuclear kinetic energy and are not carried out in either the diabatic or the adiabatic limits and Born−Oppenheimer potential surfaces are not meaningful. However, thinking in terms of the diabatic surfaces (where both transitions are allowed) and the adiabatic surfaces (where the transition to the upper surface is dipole allowed and that to the lower surface is vibronically allowed) provides a meaningful physical picture. It shows why, as the coupling increases, the absorption band contains two components that move apart in energy and differ increasingly in intensity.

c. Time-Domain Interpretation. The features of the experimental absorption spectrum can be interpreted using a time-domain picture. The crucial element to this interpretation is the time evolving wave packet, $\phi(t)$, which dictates the shape of the overlap function, $\langle\phi|\phi(t)\rangle$. Using the split operator method, we solved eq 6 for the time-dependent wave packet, $\phi(t)$. For each time step in the calculation, the 2×2 matrix operates simultaneously on $\phi_1(Q,t)$ and $\phi_2(Q,t)$. The diagonal elements move the two wave packets along the coupled potential surfaces, while the off diagonal elements transfer amplitude between the electronic states.

To visualize the time-dependent wave packet moving on the coupled surfaces, the changes that the wave packet experiences are examined at several time steps. For clarity, only the wave packet propagating on surface 2 (Figure 1) is examined. The wave packet is shown at six times ranging from 0 to 8 fs in the top part of Figure 5. Figure 5 shows that, over time, some wave packet amplitude remains centered around $Q = 0$ while part of the wave packet moves away from the Franck−Condon region toward larger distances.

The time-domain explanation for the existence of the shoulder and main peak of the absorption band is summarized by examining the short-time overlaps shown by the solid line in the bottom panel of Figure 5. The total overlap decreases rapidly, reaches a local minimum at about 3.8 fs, and then increases to

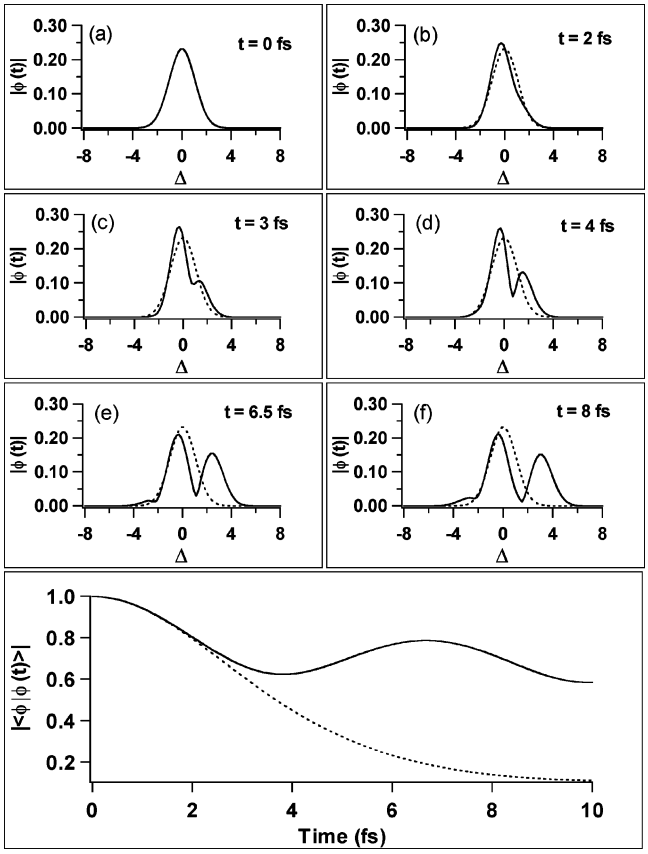

Figure 5. Top: Plots of $|\phi(t)|$ at (a) $t = 0$ fs, (b) $t = 2$ fs, (c) $t = 3$ fs, (d) $t = 5$ fs, (e) $t = 6.5$ fs, and (f) $t = 8$ fs dotted lines represent $|\phi(t)|$ at $t = 0$ fs. Bottom: Plot of the absolute value of the correlation function as a function of time for the coupled (solid line) and uncoupled (dotted line) potentials. All calculations were carried with the parameters used to calculate the spectrum in Figure 3b. Note the recurrence at $t = 6.7$ fs.

give a recurrence at about 6.7 fs. In contrast, the overlap for the uncoupled surfaces (shown by the dotted line) decreases smoothly to zero. The complicated terrain of the coupled surfaces leads to the more complicated behavior of $\phi(t)$ and thus the recurrence. When transformed to the frequency domain, the recurrence at $t = 6.7$ fs corresponds to a separation between bands in the frequency domain of $c^{-1}t^{-1} = 4975$ cm^{-1}. The net result is to produce a spectrum containing two peaks separated by 4975 cm^{-1}, as shown in Figure 3b.

4. Emission Spectra from the Mixed Valence Excited Electronic State. In this section, the calculated emission spectrum for the dication system is discussed. After a brief explanation of the steps involved in the calculation, the added constraints on the parameters used to define the excited-state mixed valence system that are imposed by fitting the experimental emission spectrum are addressed.

Using the same parameters that define the ground and excited-state surfaces for the calculation of the absorption spectrum, we obtained the lowest energy eigenfunction of the excited-state surface. After multiplying this eigenfunction by the appropriate transition dipole moment, we then propagated the resulting initial wave packet, ϕ_i, on the ground-state potential surface. The time-dependent overlap, $\langle\phi_i|\phi(t)\rangle$, is calculated and used to generate the emission spectrum. Using this procedure and the same parameters that defined the surfaces for the absorption spectrum calculation shown in Figure 3b, we calculated the emission spectrum shown in Figure 4a. The intrinsic bandwidth of the spectrum based on only the asymmetric mode is narrower than that of the experimental emission spectrum shown in Figure 2, which has a bandwidth at half-maximum of 2640 cm^{-1}. When the symmetric modes are included in the calculation, as discussed in section 5, the bandwidth is the same as that of the experimental spectrum.

The experimental emission bandwidth restricts the range of parameters that define the potential surfaces. More specifically, the emission spectrum calculation is much more sensitive to the frequency chosen to define the potential energy surfaces along the asymmetric coordinate than is the absorption spectrum calculation. Returning to the low-frequency mode example in which the excited-state diabatic frequency is 521 cm^{-1}, the same values of Δ and H_{ab}^{ex} that yielded the calculated absorption spectrum, shown in Figure 4b, are now used to calculate the emission spectrum. The intrinsic bandwidth of the calculated spectrum, also shown in Figure 4b, is larger than that of the experimental spectrum even without the inclusion of the symmetric modes. When the symmetric modes are included, the bandwidth is even larger. This restriction on the frequency used to define the potential surfaces shows that a stretching vibration rather than a low-frequency bridge-**Hy** bending mode is the relevant normal mode.

5. Final Fit Including Both Symmetric and Asymmetric Modes. The symmetric modes contribute to the bandwidth of the absorption and emission spectra. The key factor in absorption bandwidth is the slope of each excited-state surface in the Franck−Condon region. The slope is determined by both the frequency and the displacement of the potential surface along its normal coordinate. In the time domain, the steeper the slope, the faster the time-evolving wave packet moves, and thus the more rapidly the correlation function decreases. The fast decrease at short time results in a broad spectrum in the frequency domain.

For the dication, the frequencies of the excited-state surfaces along the symmetric coordinates are determined from the resonance Raman spectrum. The displacements are determined by the intensities. The simultaneous fit of the experimental absorption spectrum, the experimental emission spectrum, and the experimental resonance Raman spectrum is obtained using the same set of displaced surfaces. Six modes along symmetric coordinates are included along with the previously discussed asymmetric mode, in the calculation of the emission and absorption spectra.

The best fits of the experimental electronic spectra are obtained when both the asymmetric and the symmetric modes are included in the calculations. The optimal H_{ab}^{ex} and Δ values for the diabatic surfaces along the asymmetric coordinate are 2000 cm^{-1} and 1.55, respectively. A frequency of 1600 cm^{-1} is used to define the excited-state diabatic surfaces such that the frequency for the coupled surfaces (1448 cm^{-1}) is comparable to that of the ground-state surface (1462 cm^{-1}). The frequencies and displacements of the symmetric mode surfaces are as follows: 350 cm^{-1} ($\Delta = 1.48$); 1015 cm^{-1} ($\Delta = 0.39$); 1181 cm^{-1} ($\Delta = 0.33$); 1305 cm^{-1} ($\Delta = 0.54$); 1413 cm^{-1} ($\Delta = 0.40$); 1552 cm^{-1} ($\Delta = 0.57$). These dimensionless displacements of the high frequency modes represent bond length changes that are consistent with those associated with C−C and C−N stretching modes of similar durene bridged molecules. For the calculated fit of the room-temperature absorption

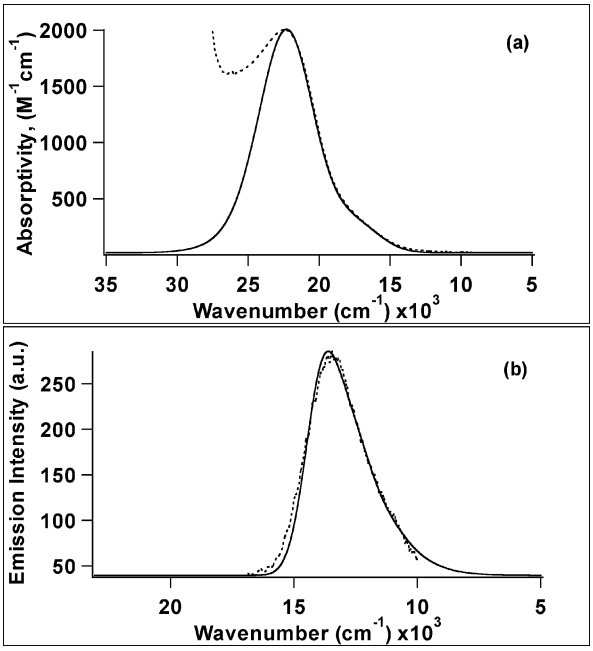

Figure 6. Best fit of the absorption spectrum (top) and emission spectrum (bottom) superimposed on the corresponding experimental spectra (dotted lines). The spectra are calculated using both the asymmetric and the symmetric vibrational modes, and the frequencies and displacements given in the text.

spectrum, $\Gamma = 1110$ cm^{-1}, and for the fit of the 15 K emission spectrum, $\Gamma = 450$ cm^{-1}.

As shown in Figure 6a, the resulting calculated absorption spectrum possesses the dominant peak around 22 000 cm^{-1} and shoulder at lower energy, and also the bandwidth of the experimentally observed spectrum. If the symmetric modes are used alone (without the asymmetric mode), the characteristic shoulder is absent. The combination of the symmetric and asymmetric modes is required to produce the overall bandwidth and band shape. The calculated emission spectrum, shown in Figure 6b, possesses an appropriate bandwidth that fits the experimental spectrum.

A delicate balance of the parameters involved in these calculations is required to obtain a simultaneous fit to the experimental absorption and emission spectra. Specifically, the calculated spectra need to reproduce the position and relative intensities of the peak maximum and shoulder of the experimental absorption spectrum along with the width of both the emission and the absorption spectra. For the asymmetric coordinate, only a narrow range of H_{ab}^{ex} and Δ values that define the excited-state mixed valence surfaces will accommodate these fitting requirements; changing H_{ab}^{ex} by more than ± 100 cm^{-1} and Δ by more than ± 0.1 results in significantly poorer calculated spectra.

Both H_{ab}^{ex} and Δ influence the electronic spectra, but the absorption spectrum is most sensitive to the coupling and the emission spectrum is most sensitive to the displacement. For the absorption spectrum calculation, the coupling influences both the energy separation and the intensity ratio between the dominant peak and its lower energy shoulder. For example, a large H_{ab}^{ex} value leads to a greater energy separation and a larger intensity ratio between the two features of the absorption band. The emission spectrum, however, is more influenced by the displacement of the surfaces than the coupling between them. A large Δ value for the surfaces along the asymmetric coordinate yields an emission spectrum with a large bandwidth. For the best fit to both the absorption and the emission spectra, a value of H_{ab}^{ex} that yields the appropriate band shape of the calculated absorption spectrum must be used in conjunction with a value of Δ that produces a suitable bandwidth in the calculated emission spectrum. All of the spectra are fit using a single set of parameters that define all of the surfaces involved in the calculations.

On the basis of the values of the parameters obtained by fitting the spectrum, the value of the coupling between the two-electron sites in the excited state of the dication can be compared with that between the one-electron sites in the monocation, and the reorganization energy, λ, can be calculated. The H_{ab}^{ex} in $\mathbf{1}^{2+}$ is about 2000 cm^{-1}, about 50% larger than the H_{ab} of 1320 cm^{-1} obtained for the ground state of $\mathbf{1}^{2+}$. Because the increment in λ_v for a mode of frequency $h\nu_q$ is $^1/_2\Delta_q{}^2 h\nu_q$, the vibrational contributions to λ for the intervalence transition of $\mathbf{1}^{2+}$ are about 1760 cm^{-1} for the unsymmetrical mode and a total of 1468 cm^{-1} for the symmetrical modes. Because the u and l surfaces lie 22 400 and 18 400 cm^{-1} above the ground-state surface in acetonitrile, $\lambda + \Delta G°$ for the transition is 20 400 cm^{-1}, and $\lambda_s + \Delta G°$ corresponds to 17 000 cm^{-1} (2.1 eV).

The calculated absorption band for $\mathbf{1}^{2+}$ (Figure 6a) allows more quantitative testing of the relationship between the magnetic superexchange coupling (J) of the dication, a two-electron interaction, and the intervalence electron-transfer coupling (H_{ab}) of the monocation, a one-electron interaction, which was first postulated by Kramers in 1934.[35] Because only a singlet diradical can have superexchange stabilization, the dication superexchange band optical spectrum was postulated to be quantitatively related to the singlet, triplet energy gap. Using the simplest theory and ignoring H_{ab}^{ex}, we previously determined that the singlet, triplet energy gap $2J$ would be related to the optical spectrum by eq 15,[7] written here in the nomenclature of this paper,

$$|J| = [H_{g(lu)}(\mathbf{1}^{2+})]^2/E_a(\mathbf{1}^{2+}) = [\mu_{g(lu)}(\mathbf{1}^{2+})/ed]^2/E_a(\mathbf{1}^{2+}) \quad (15)$$

where the g(lu) subscript now refers to the ground state to both lower (l) and upper (u) components of the excited state energy surface (see Figure 1) μ is the transition dipole moment and H is the electronic interaction. The calculated absorption spectrum (Figure 6, top), which includes both components, has band maximum $E_a(\mathbf{1}^{2+}) = 22\,315$ cm^{-1} and $\mu_{g(lu)} = 1.96$ D using Liptay's formulation of the equation for calculating the transition dipole moment.[36] We previously used the Hush Gaussian approximation to obtain μ for the obviously non-Gaussian band of $\mathbf{1}^{2+}$,[7] which is clearly inadequate for quantitative testing, and produced a smaller transition dipole moment. When used with an estimated electron transfer distance, d, of 5.75 Å, a value of $H_{g(lu)} = 1580$ cm^{-1} is obtained, which is 1.49 times the experimental monocation $H_{ab}(\mathbf{1}^{+})$ value of 1070 cm^{-1},[37] slightly larger than the predicted statistical ratio of $2^{1/2} = 1.41$. The eq 15 value for J is 112 cm^{-1}, which is larger than the SQUID value of 72 cm^{-1}.[7]

(35) For a review, see: Anderson, P. W. In *Magnetism*; Rado, G. T., Suhl, H., Eds.; Academic Press: New York, 1965; Vol. 1, Chapter 2, p 25.
(36) Liptay, W. *Angew. Chem., Int. Ed. Engl.* **1969**, *8*, 177.
(37) Nelsen, S. F.; Trieber, D. A., II; Ismagilov, R. F.; Teki, Y. *J. Am. Chem. Soc.* **2001**, *123*, 5684.

Summary

The lowest energy excited state of the **Hy2Du**$^{2+}$ ($\mathbf{1}^{2+}$) cation arises from a transition from the ground state where one positive charge is associated with each of the hydrazine units to an excited state where both charges are associated with one of the hydrazine units. The transition can be considered to be a **Hy**-to-**Hy** charge transfer, and, in its excited state, the molecule is a Class II mixed valence system in which the charges on the charge-bearing units differ by two instead of by one as they do in ground-state mixed valence molecules. The lowest energy absorption band is asymmetric with weak low-energy shoulder and an intense higher energy peak. Both the shoulder and the peak are a consequence of the transition to the coupled excited state. Emission from the lowest energy vibronic level of the coupled excited state to the ground state is observed at low temperature. Band intensities in the resonance Raman spectra are used to determine the displacements of the totally symmetric normal modes. The absorption, emission, and resonance Raman spectra are calculated simultaneously by using the seven-dimensional potential energy surfaces.

The details of the absorption and emission spectra are calculated by using the time-dependent theory of spectroscopy and methodology designed to calculate spectra involving coupled surfaces. The calculations are carried out in the diabatic basis, but the nuclear kinetic energy is explicitly included and the calculations are exact quantum calculations of the model Hamiltonian. The absorption process creates a wave packet on the excited coupled surfaces. The transition involves the transfer of an electron from the hydrazine on one side of the molecule to the hydrazine on the other side and vice versa. The two transitions are antiparallel, and the transition dipole moments have opposite signs. Upon transformation to the adiabatic basis, the dipole moment for the transition to the highest energy adiabatic surface is almost constant, but that for the transition to the lowest surface is zero at the ground-state internuclear separation. The latter dipole moment is nonzero at other positions along the vibrational coordinate and changes sign at the origin; this dipole represents a vibronically allowed transition. The energy separation between the two components of the absorption spectrum is twice the coupling between the diabatic basis states.

The bandwidths of the electronic spectra are caused by unresolved progressions in totally symmetric modes as well as progressions in the modes along the coupled coordinate. The totally symmetric modes are modeled as displaced harmonic oscillators; the frequencies and displacements are determined from resonance Raman spectra.

The quantities that best fit the absorption, emission, and Raman spectra simultaneously are severely constrained by the experimental spectra. The best fit is obtained by using a frequency appropriate for a stretching mode rather than a bending mode for the asymmetric coordinate. Low-frequency bending modes cannot simultaneously fit the observed absorption and emission bandwidths. The coupling is determined from the absorption spectrum and the contributions of the symmetric modes from the resonance Raman spectra.

Excited-state mixed valence, although not investigated in detail until now, is expected to be an important contributor to the electronic spectra of many organic and inorganic compounds. For example, in uncharged molecules that are otherwise similar to the one studied here, the lowest excited states may involve coupled mixed valence species that can be represented as pairs of nitrogen cations and bridge anions. When the energy separations and relative intensities enable the excited-state properties to be calculated, the spectra will provide new information for probing and understanding coupling in mixed valence systems.

Acknowledgment. This work was made possible by grants from the National Science Foundation (CHE 0206857 to J.I.Z., CHE-9988727 to S.F.N.).

JA036046K